Optimization and Performance Evaluation of Organic Rankine Cycle Configurations Using Various Working Fluids

Milad Sohrabi^a, Majid Ahmadian^b

^aStudent number : 402211297, Msc. Process Design in Chemical Engineering , Sharif university of Technology ^bStudent number : 402200694, Msc. Process Design in Chemical Engineering , Sharif university of Technology

Abstract

The Organic Rankine Cycle (ORC) offers a promising solution for converting low-grade heat into electricity by utilizing organic fluids with favorable thermodynamic properties. This study explores the impact of different working fluids on ORC efficiency across various configurations. Through experimental and simulation analyses, the study identifies R142b, FC-72 and dichloromethane as top performers under different conditions. Results demonstrate that fluid selection critically influences ORC performance. This research underscores the ORC's versatility in enhancing energy efficiency and reducing waste across industrial applications.

Keywords: Rankine Cycle, GAMS, Fluid selection;

I. INTRODUCTION

The Organic Rankine Cycle (ORC) represents a significant advancement in power generation technology, leveraging low-grade heat sources for the production of electricity. Named after its working principle derived from the conventional Rankine cycle, the ORC differentiates itself by employing organic fluids with favorable thermodynamic properties instead of water. This adaptation allows the ORC to efficiently exploit heat from diverse and typically low-temperature sources, such as geothermal reservoirs, solar thermal energy, industrial waste heat, and biomass combustion.

The selection of an appropriate working fluid is a critical aspect of optimizing ORC performance. The ideal fluid must possess several key characteristics to ensure efficiency and safety. These include

suitable boiling and condensation points relative to the heat source and sink, high thermal stability, low viscosity, and minimal environmental impact. Additionally, the fluid should exhibit a high molecular weight and density, which contribute to higher cycle efficiency and lower volumetric flow rates.

Evaluating potential working fluids involves a comprehensive analysis of their thermophysical properties and compatibility with system components. refrigerants, Fluids such as hydrocarbons, and siloxanes are considered due to their varied boiling points and thermal properties. Moreover, the environmental and safety considerations, such as global warming potential (GWP) and flammability, are integral to the selection process.

In summary, the ORC's adaptability to low-temperature heat sources and the judicious choice of working fluid renders it a versatile and sustainable option for enhancing energy efficiency and mitigating waste. Continued research and development in this field aim to refine fluid selection criteria and expand the applicability of ORC technology across various industrial sectors.

Abbas et al. [1] experimentally examined a cascaded two-Organic Rankine Cycle (ORC) system across various temperatures and pressures to optimize performance. Cyclopentane was used in the high-temperature (HT) cycle, while pentane, butane, and propane were tested in the low-temperature (LT) cycle. Results highlighted that pentane maximized heat transfer, absorbing 23 kW, but most heat from the HT cycle was not transferred to the LT cycle.

Yu et al. [2] focuses on optimizing the design and operation of a solar energy-driven ORC system utilizing a parabolic trough collector and a two-tank sensible thermal energy storage system. Results showed that a recuperative ORC significantly outperforms a basic ORC, with toluene emerging as the best working fluid despite vacuum condensation issues.

Abbas et al. [3] explored the thermal efficiency of a Cascaded Dual-Organic Rankine Cycle (CD-ORC) system using alkanes and low-GWP refrigerants through simulations with EBSILON@Professional. The analysis revealed that thermal efficiency in the HT-ORC is influenced by the critical temperature, molecular mass, and critical pressure of the working fluids, with cyclic alkanes like cyclohexane showing superior performance. In the LT-ORC, refrigerants with high critical temperatures, such R1366mzz(Z) and R1233zd(E), achieved the highest efficiency. The CD-ORC system demonstrated a potential 25% efficiency improvement over regular ORC systems.

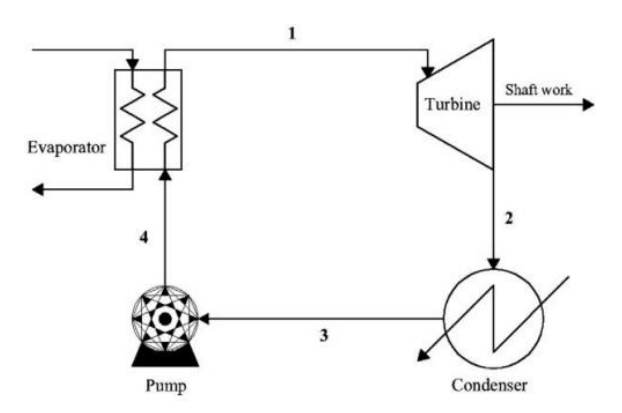


Figure 1. Rankine cycle for Config. A [4]

In the following, the thermodynamic modeling of the ORC (Organic Rankine Cycle) is examined. To model this cycle using various assumptions, three different approaches for the thermodynamic simulation of the cycle showen in Figure 1.

II. CONFIGURATION A – APPROACH 1

To model the thermodynamics of Figure 1 using Approach 1, which is based on obtaining the enthalpy of different streams, assumptions include: the turbine outlet pressure is 1 bar, zero pressure drop for equipment, a minimum temperature approach of 5°C for cycle heat exchangers, an evaporator outlet temperature of 165°C, purity of each stream, condenser outlet temperature slightly less than the boiling point of the substance, a 1°C temperature increase across the pump, 75% pump efficiency, 80% turbine isentropic efficiency, 95% electric motor efficiency, and operational constraints such as the turbine inlet being fully vapor and the turbine outlet having a steam quality that can decrease to 90% as mentioned in [2]. The specifications of the hot water flow rate are given in Table 1.

Table 1. Waste Water property

| rable 1: waste water property | | |
|-------------------------------|------------|--|
| Parameter | Value | |
| Pressure | 10 bara | |
| Temperature | 170 °C | |
| Flowrate | 100 kg/s | |
| Composition | Pure Water | |

To determine the enthalpy of each stream, Equation 1 is used. The actual enthalpy of each stream includes three to four parameters: the ideal gas enthalpy, the residual enthalpy indicating the deviation from the ideal state, the formation enthalpy which is a constant value for the substance, and if the substance is in the liquid phase, the enthalpy of vaporization should be added to the actual enthalpy.

$$H^{real} = H^{ig} + H^{res} + H^{form} + H^{vap}$$
 eq. 1

If the stream is two-phase, Equation 2 must be used, which calculates the enthalpy for saturated vapor and liquid, and then the vapor fraction of the stream is inserted into the equation to obtain the actual enthalpy.

$$H = vap. frac * H^{Sat.vap} + (1 - vap. frac) * H^{Sat.liq} eq. 2$$

To calculate the ideal gas enthalpy of a stream, Equation 3 is used. Coefficients a to f are read from the Aspen HYSYS software, and by inputting the temperature in Kelvin into Equation 3, the ideal gas enthalpy (Kj / Kg) is obtained.

$$H^{ig} = a + bT + cT^2 + dT^3 + eT^4 + fT^5$$
 eq. 3

To calculate the second parameter in Equation 1, the residual enthalpy, existing EOS ¹ are used. Considering the problem's requirements, the PR² equation of state is chosen. Using the relations provided in [5], presented as Equations 4 to 12, the desired parameter is calculated. To solve the cubic equation in Equation 5, the Kamath method is used.

$$H^{Res} = RT \left(Z - 1 - \frac{A}{B\sqrt{8}} \left(1 + \frac{m\sqrt{T_r}}{\sqrt{\alpha}} \right) ln \left[\frac{Z + (1 + \sqrt{2})B}{Z + (1 - \sqrt{2})B} \right] \right) \quad \text{eq.} 4$$

$$Z^3 - (1 - B)Z^2 + (A - 2B - 3B^2)Z - (AB - B^2 - B^3)$$
 eq.5

$$T_r = \frac{T}{T_c}$$
 eq.6

$$\alpha = \left[1 + m(1 - T_r^{0.5})\right]^2$$
 eq.7

$$m = 0.375 + 1.54\omega - 0.27\omega^2$$
 eq.8

$$a = 0.457235 \frac{R^2 T_C^2}{P_C} * \alpha$$
 eq.9

$$b = 0.077796 \frac{RT_C}{P_C}$$
 eq.10

$$A = \frac{aP}{(RT)^2}$$
 eq.11

$$B = \frac{bP}{RT}$$
 eq.12

Assuming the purity of each stream, by substituting either the temperature or pressure of a stream, other parameters of that stream, such as the fugacity coefficient (Equations 13 & 14) or the compressibility factor, can be calculated.

for pure system
$$\rightarrow \varphi^v = \varphi^l$$
 eq.13

$$\ln(\varphi) = (z - 1) - \ln(z - B) + \frac{A}{2B\sqrt{2}} \ln\left(\frac{z + (1 - \sqrt{2})B}{z + (1 + \sqrt{2})B}\right) \quad \text{eq.} 14$$

To find the molar flow rate of the pure component in the cycle, Equation 15 is used, which determines the molar flow rate of the component by balancing the energy in the cycle's evaporator.

$$\dot{n}(H_1 - H_4) = \dot{m}_w C_{p,w} (\Delta T - 5)$$
 eq. 15

Subsequently, the thermodynamic parameters of the mentioned cycle are calculated, and the pump's required work is determined using Equation 16 & 17. Finally, the turbine's generated work is calculated using Equation 18.

¹ Equations of State

² Peng Robinson

$$\Delta H_{pump} = \frac{(P_4 - P_3) * \dot{n} * MW}{density} \qquad eq. 16$$

$$W_{pump} = \frac{\Delta H_{pump}}{\eta_{pump}} \qquad eq. 17$$

$$W_{turbine} = \dot{n}(H_1 - H_2) \qquad eq. 18$$

To select among the 74 components listed in the provided Excel file, two constraints are applied: the condenser outlet temperature must be at least 30°C, and the selected component must have a boiling point lower than water. By applying these constraints, 15 components listed in Table 2 are identified as candidates for the best substance for this cycle.

Table 2. Candidates for best component

| Working Fluid | | | | |
|--------------------|-----------|-----------|--|--|
| 2,2-dimethylbutane | FC72 | R113 | | |
| 4-methyl-2-pentene | Isohexane | Benzene | | |
| Acetone | Methanol | Ethanol | | |
| Cyclopentane | n-hexane | n-heptane | | |
| Dichloromethane | n-pentane | R141b | | |

In this approach, five components - dichloromethane, FC-72, methanol, n-heptane, and R-113 - are selected.

III. CONFIGURATION A – APPROACH 2

In Approach 2, similar to the previous case, the mentioned relations and assumptions are used, with the difference that the turbine outlet is assumed to be saturated vapor at 1 bar pressure, ensuring no liquid forms inside the turbine. Therefore, only the vapor enthalpy is used, resulting in reduced generated work. The same components as in Approach 1 are used in Approach 2.

IV. CONFIGURATION A – APPROACH 3

In Approach 3, the general relations of the previous two approaches are used, with the difference that since only dichloromethane converts

to approximately 94% liquid, and the other components remain in their gaseous state, the vapor fraction of this component is included in the equations. Additionally, using Equation 19 [6], the turbine outlet temperature is calculated considering the pressure drop and the K value, which equals C_p/C_v of the component in the ideal state, and the turbine's isentropic efficiency equal to 80%. The components used in the Approach 3 are the same as those in the previous two approaches.

$$\eta_{turbine} = \frac{1 - \frac{T_2}{T_1}}{1 - \pi_i^{\frac{1-k}{k}}}$$
 $eq. 19$

V. CONFIGURATION B

In the Bonus section of this project, the performance comparison among five components - isohexane, FC-72, R-113, dichloromethane, and R-141b - is conducted. This section follows the structure shown in Figure 2.

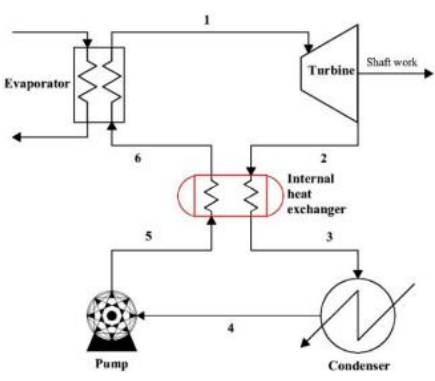


Figure 2. Configuration B[4]

The assumptions used in this section are similar to those of Approach 3 in Configuation 1, with the difference that the pump outlet temperature is considered to be 304.15 K to maintain the 5°C approach temperature for the middle heat exchanger in Figure 2. With this assumption, the minimum approach temperature for all candidate components is met. Also, the UA values are derived from [7] considering the water-organic fluid type, and the required area for the cycle's evaporator is determined and substituted into the equations. In this section, similar to the previous sections, the

primary task is to calculate the actual enthalpy of the cycle streams, assuming the turbine inlet stream is at 165°C and in the saturated vapor state. By calculating the enthalpy of streams 1, 6, 2, 5, and 4 and using two additional relations compared to the previous approaches, 20, 21 and 22, the turbine work, cycle work, and all required parameters are determined and calculated.

$$H_6 - H_5 = H_3 - H_2$$
 eq. 20

$$U * A * f * LMTD = \dot{m}_w C_{p,w}(\Delta T)$$
 eq. 21

$$LMTD = \frac{(T_{in,waste} - T_1) - (T_{out,waste} - T_6)}{\ln \frac{(T_{in,waste} - T_1)}{(T_{out,waste} - T_6)}}$$
eq.22

VI. RESULTS & DISCUSSION

The results obtained from configuration A-Approach 1 are presented in Table 3. Comparing these results with the simulations conducted in Aspen HYSYS, it is observed that FC72, with a net work production of 21296 kW, exhibits the highest work output among the candidate components listed in Table 2. Table 3 also highlights the differences between the results obtained from the model in GAMS software and the simulation results from Aspen HYSYS. It is evident that the modeling results closely match the HYSYS simulation outcomes, with an average error percentage of 0.32%, showing the results verified and acceptable.

Table 3. Config.A approach 1 Results

| Tuest et estiligir approuen i ressures | | | |
|--|----------|----------|---------|
| Spec | Model | HYSYS | Error % |
| W _{pump} (KW) | 311.66 | 312.4 | 0.24% |
| W _{turbine} (KW) | 22639.9 | 22616 | 0.11% |
| n (mole/s) | 0.8202 | 0.8212 | 0.12% |
| P1 (bar) | 13.65 | 13.657 | 0.05% |
| T2 (K) | 332.7 | 332.9 | 0.06% |
| T4 (K) | 330 | 329.9 | 0.03% |
| H1 (Kj/Kmol) | -2932254 | -2932305 | 0.00% |
| H2 (Kj/Kmol) | -2959858 | -2959825 | 0.00% |

| H4 (Kj/Kmol) | -2986405 | -2986691 | 0.01% |
|----------------|----------|----------|-------|
| Z factor 1 | 0.5007 | 0.5004 | 0.06% |
| Z factor liq 2 | 0.0084 | 0.00821 | 2.32% |
| Z factor Vap 2 | 0.9367 | 0.9367 | 0.00% |
| Z factor 4 | 0.1131 | 0.1117 | 1.25% |

Additionally, the results for the other two approaches are presented in Tables 4 and 5. Approach 2 achieves an average error percentage of 0.35%, and Approach 3 has an average error percentage of 0.57%, both yielding reliable and valid results.

Table 4. Config.A approach 2 Results

| 1 dole 1. Comig.11 approach 2 Results | | | |
|---------------------------------------|----------|------------|---------|
| Spec | Model | HYSYS | Error % |
| W _{pump} (KW) | 311.54 | 312.4 | 0.28% |
| W _{turbine} (KW) | 20290.6 | 20255 | 0.18% |
| n (mole/s) | 0.8202 | 0.8218 | 0.19% |
| P1 (bar) | 13.65 | 13.657 | 0.05% |
| T2 (K) | 332.4 | 332.9 | 0.15% |
| T4 (K) | 330 | 329.9 | 0.03% |
| H1 (Kj/Kmol) | -2932254 | -2932304.7 | 0.00% |
| H2 (Kj/Kmol) | -2956995 | -2956943.3 | 0.00% |
| H4 (Kj/Kmol) | -2986405 | -2986691.3 | 0.01% |
| Z factor 1 | 0.5007 | 0.5004 | 0.06% |
| Z factor liq 2 | 0.0084 | 0.00821 | 2.32% |
| Z factor Vap 2 | 0.9367 | 0.9367054 | 0.00% |
| Z factor 4 | 0.1131 | 0.1117 | 1.25% |

Consequently, in the modeling of Approach 2, FC72 is identified as the selected component with a net work production of 18964 kW. However, in Approach 3, given the assumptions made, dichloromethane is determined to be the selected component with a net work production of 8029 kW. The comparison of the results from Approaches 1 and 2 confirms that components with higher molecular weight and density exhibit superior performance in the Rankine cycle. Furthermore, the results from Approach 3 indicate that components with a vapor fraction less than one, or at their saturation point, perform better in the Rankine cycle compared to their superheated state.

Table 5. Config.A approach 3 Results

| | , U | | |
|---------------------------|---------|----------|---------|
| Spec | Model | HYSYS | Error % |
| W _{pump} (KW) | 240.62 | 242.6 | 0.82% |
| W _{turbine} (KW) | 8705.6 | 8695 | 0.12% |
| n' (mole/s) | 1.3937 | 1.389 | 0.34% |
| P1 (bar) | 20.97 | 20.95 | 0.10% |
| T2 (K) | 312.88 | 312.4 | 0.15% |
| T4 (K) | 314 | 313.1 | 0.29% |
| H1 (Kj/Kmol) | -90083 | -90100.7 | 0.02% |
| H2 (Kj/Kmol) | -96330 | -96359.9 | 0.03% |
| H4 (Kj/Kmol) | -121951 | -122277 | 0.27% |
| Z factor 1 | 0.7546 | 0.7549 | 0.04% |
| Z factor liq 2 | 0.0026 | 0.00253 | 2.81% |
| Z factor Vap 2 | 0.9753 | 0.975241 | 0.01% |
| Z factor 4 | 0.0541 | 5.28E-02 | 2.46% |

In examining the results for Configuration B, presented in Table 6, it is observed that R141b, with a net work production of 8463 kW, outperforms the other candidates listed in Table 2. Comparing the selected component in Approach 3 of Configuration A with the results obtained in Configuration B reveals that dichloromethane in Configuration A performs better than R141b, placing R141b as the second-best component. However, in Configuration B, the positions of these two components are reversed. The reason for this is that dichloromethane exits the turbine at its saturated vapor temperature, while R141b exits in a superheated state, allowing for thermal exchange with the pump's discharge stream.

Table 6. Config.B Results

| Spec | Model | HYSYS | Error % |
|------------|----------|--------|---------|
| n (mole/s) | 1.3976 | 1.392 | 0.40% |
| P1 (bar) | 23.4233 | 23.44 | 0.07% |
| Z factor 2 | 0.9752 | 0.9751 | 0.01% |
| T2 (K) | 334.5349 | 333.8 | 0.22% |
| T5 (K) | 304.15 | 304.6 | 0.15% |
| Z factor 5 | 0.0826 | 0.0886 | 6.73% |
| T4 (K) | 303.15 | 303.1 | 0.02% |
| Z factor 4 | 0.0036 | 0.0038 | 5.34% |

| T6 (K) | 328.7977 | 328.8 | 0.00% |
|---------------------------|----------|---------|-------|
| H1 (Kj/Kmol) | -329923 | -329948 | 0.01% |
| Z factor 1 | 0.6537 | 0.6535 | 0.03% |
| H6 (Kj/Kmol) | -361905 | -362069 | 0.05% |
| Z factor 6 | 0.0796 | 0.0853 | 6.73% |
| H2 (Kj/Kmol) | -336599 | -336669 | 0.02% |
| H5 (Kj/Kmol) | -365133 | -365242 | 0.03% |
| H4 (Kj/Kmol) | -362815 | -365529 | 0.74% |
| H3 (Kj/Kmol) | -333371 | -339842 | 1.90% |
| W _{pump} (KW) | 400.54 | 399.1 | 0.36% |
| W _{turbine} (KW) | 9330.12 | 9351 | 0.22% |

VII. CONCLUSION

The performance evaluation of different working fluids in ORC systems reveals significant insights into optimizing energy efficiency. The experimental studies and simulations demonstrate that the selection of appropriate working fluids, such as cyclopentane, FC-72, and dichloromethane, is crucial for maximizing the efficiency of ORC configurations. The findings show that FC-72 consistently achieved the highest net work output across different approaches, emphasizing the importance of molecular weight and density in fluid performance. The comparison between various configurations also highlights that fluids exiting the turbine in a saturated vapor state perform better than those in a superheated state, due to enhanced thermal exchange capabilities.

References

- [1]: Wammedh Khider Abbas, Experimental Study of two cascade.., 2021.
- [2]: Haoshui Yu, Optimal design and operation, 2021.
- [3]: Wammedh Khider Abbas, Cascaded dual-loop organic..., 2021.
- [4]: Palma-Flores, O., Flores-Tlacuahuac, A., & Canseco-Melchor, G. (2015)
- [5]: Lee, computional method in chemical eng, 2019.
- [6]: stlukes-glenrothes.org
- [7]: biegler & grossmann, systematic methods, 1997.